



Article

Pull-Out Resistance of Rebar Stake Depending on Installation Conditions and Compaction Levels of Agricultural Soil

Giseok Heo ¹, Inhyeok Choi ¹, Jinyoung Lee ¹, Heedu Lee ², Seongyoon Lim ³ and Dongyoun Kwak ^{1,*}

¹ Department of Civil and Environmental Engineering, Hanyang University, ERICA, Sangnok-gu, Ansan 15588, Republic of Korea; gsheo@hanyang.ac.kr (G.H.); ssonagbi11@hanyang.ac.kr (I.C.); jylee84@hanyang.ac.kr (J.L.)

² Department of Architectural Engineering, Kyungpook National University, Daegu 41566, Republic of Korea

³ Department of Agricultural Engineering, National Institute of Agricultural Sciences, Rural Development Administration, Jeonju 54875, Republic of Korea; limsy73@korea.kr

* Correspondence: dkwak@hanyang.ac.kr; Tel.: +82-31-400-5141

Abstract: Strong winds, particularly in the absence of disaster-resistant designs, significantly impact the stability of greenhouse foundations and eventually lead to structural damage and potential harm to crops. As a countermeasure, rebar stakes are commonly used to reinforce the foundations of non-disaster-resistant greenhouses. This study evaluates the pull-out resistance ($R_{pull-out}$) of rebar stakes considering various factors like soil compaction, embedded length, installation duration and angle, and changes in soil water content against uplift pressure by strong winds. A combination of field (i.e., the cone penetration test and rebar stake pull-out test) and laboratory (i.e., the compaction test, soil compaction meter test, and soil box test) tests are performed for the assessment of $R_{pull-out}$. The results indicate that $R_{pull-out}$ increases with higher soil compaction, greater embedded length, longer installation duration, and an inclined installation angle. The soil compaction exerts the most significant impact; 90% to 100% of the soil compaction rate has approximately 10 folds higher $R_{pull-out}$ than the 60–70% compaction rate. If the embedded length is increased from 20 cm to 40 cm, there is a two-fold increase in the average of $R_{pull-out}$. Inclined installation of rebar stakes increases $R_{pull-out}$ by 250% to 350% compared to vertical installation, and rebar stakes installed prior to the uplift event have 1.5 to 6.4 fold increases in $R_{pull-out}$ than those with instant installation. Additionally, we observed variations in the surface soil moisture due to climatic changes introducing variability in $R_{pull-out}$. These findings lead to the proposition of efficient rebar stake installation methods, contributing to the enhanced stability of a greenhouse.

Keywords: pull-out resistance; rebar stake; greenhouse foundation; soil water content; soil hardness



Citation: Heo, G.; Choi, I.; Lee, J.; Lee, H.; Lim, S.; Kwak, D. Pull-Out Resistance of Rebar Stake Depending on Installation Conditions and Compaction Levels of Agricultural Soil. *Horticulturae* **2024**, *10*, 277. <https://doi.org/10.3390/horticulturae10030277>

Academic Editor: Anoop Kumar Srivastava

Received: 30 January 2024

Revised: 6 March 2024

Accepted: 11 March 2024

Published: 13 March 2024



Copyright: © 2024 by the authors. Licensee MDPI, Basel, Switzerland. This article is an open access article distributed under the terms and conditions of the Creative Commons Attribution (CC BY) license (<https://creativecommons.org/licenses/by/4.0/>).

1. Introduction

Plastic greenhouses, with their lightweight structure, are particularly susceptible to wind damage. This vulnerability has induced numerous studies focusing on their safety under wind pressure, examining how such forces impact their structural integrity [1,2]. During the summer season (June to August), typhoons often hit South Korea, accompanied by substantial rainfall [3,4]. The significance of this heavy rainfall with wind pressure cannot be understated, especially in terms of its impact on the stability of the greenhouse foundations [5]. Yoon et al. [6] noted that the primary cause of typhoon damage to greenhouses was the inadequate installation of the foundations compared to the uplift forces exerted by strong winds. Excessive moisture due to rainfall weakens the soil's shear strength, even increasing the risk of damage through uplift or overturning by strong winds [7]. This highlights the need for robust foundation designs and installation methods to ensure the resilience of plastic greenhouses against wind hazards.

In South Korea, wind hazards have led to significant damage, with 1040 ha greenhouses affected in 2020 and 7151 ha in 2021 [8]. Between 2020 and 2021, the annual financial

loss due to this damage amounted to KRW 4.4 billion [8]. This recurring problem has become a major concern for greenhouse owners and farmers. In response, the Rural Development Administration (RDA) in South Korea introduced new disaster-resistant design criteria in 2010 to mitigate the hazard. These new criteria focus on preventing uplift failure due to wind pressure and structural failure due to snow weight [9]. A key requirement of the criteria is the installation of a continuous pipe foundation at a depth of over 20 cm. This buried continuous pipe foundation is connected to greenhouse rafters, and the foundation effectively resists uplift pressure. It is reported that greenhouses adhering to these new standards have suffered minimal damage, even in strong winds [9]. However, many greenhouses were constructed before the disaster-resistant criteria were established or were not in compliance due to cost considerations. As of 2023, more than 50% of greenhouses in South Korea do not meet the new disaster-resistant standards. These non-disaster-resistant greenhouses rely only on rafter pipes buried in the ground for uplift resistance, which may be inadequate against strong winds. Some non-disaster-resistant greenhouses are reinforced using rebar stakes, but the effectiveness of rebar stakes has not been thoroughly evaluated.

Previous studies have examined various greenhouse foundation systems [10–24]. In South Korea, several studies examined the pull-out resistance of continuous pipe foundations compared with other types of foundations using a soil container [25–27]. Lim et al. [26] evaluated the pull-out resistance of continuous pipe foundations, spiral foundations, and top foundations with varying embedment depths and the soil types (i.e., silty sand, low plasticity silt, and clayey sand). They found no significant correlation between the type of soil and the foundation's pull-out resistance [26]. Song et al. [27] assessed the pull-out resistance of continuous pipe foundations, spiral foundations, and independent concrete foundations with varying soil types and compaction levels. They found that the maximum pull-out resistance was highest for the independent concrete foundations, followed by continuous pipe foundations and spiral foundations [27]. Choi et al. [25] tested the pull-out resistance of continuous pipe foundations and rafter pipes with various soil types (rice pad soil and reclaimed land soil), compaction rates, and embedment depths. The higher the compaction rate and the deeper the embedment depth, the greater the pull-out resistance for all foundations and soil types. The pull-out resistance of the continuous pipe foundation was approximately six times greater than that of one of the rafter pipes. For both types of foundations, the differences in capacities between the two soil types were not significant. Choi et al. [25] reported that if a higher compaction rate is applied, the continuous pipe foundation will be effective against pull-out force regardless of soil type. Lee et al. [16] used a numerical analysis to evaluate the pull-out resistance of continuous pipe foundations, individual pipe, spiral foundations, and top foundations under uplift load and stated that greenhouses using individual pipe foundations require essential reinforcement.

For greenhouses in Spain, three types of foundations (i.e., piles with full-length concrete, free-base anchorage, and piles with partial-length concrete) were tested against the pull-out force in the field, and numerical simulations were performed [18]. Similar to other studies, the pull-out resistance increased with the embedment depth and foundation diameter. Among the three types of foundations, they found that the pile with a full length of concrete was the most effective, and the free-base anchorage was the worst. If the length-to-diameter ratio was less than 9.5, a small displacement was observed for the concrete pile.

These previous studies often focused on continuous pipe foundations or specific foundations, limiting their relevance for non-disaster-resistant greenhouses that commonly rely on rebar stakes for pull-out resistance. The relationship between water content, compaction level, and the pull-out resistance of rebar stakes remains underexplored. In addition, for the rafter pipe, only the vertical pull-out capacity was examined, but capacities with inclined angles were not investigated. To overcome the lack of information, this study aims to develop a comprehensive understanding of the pull-out resistance of rebar stakes under varying soil conditions and installation parameters (i.e., installation length and angle).

We investigated how the soil water content and compaction level, along with installation conditions, influence the rebar stake pull-out resistance using multiple series of laboratory and field tests. Based on the test results, we suggest an optimal installation method for rebar stakes and anticipated pull-out resistance.

2. Materials and Methods

2.1. Surface Soil Types

In determining the soil types for laboratory and field testing in this study, we first assessed the distribution of surface soil types in South Korea. The National Institute of Agricultural Sciences (NIAS) provides GIS-based maps detailing surface soil conditions for agricultural purposes [28]. Among them, there are soil classification maps at very shallow depth (0–20 cm) and moderately shallow depth (20–100 cm), according to the USDA soil classification system [29]. The soil classification map for shallow depth (20–100 cm) and proportion of soil classification are shown in Figure 1. Our analysis of the map revealed that most of the soil, accounting for 75%, falls under the categories of loam or sandy loam (silty sand (SM) or clayey sand (SC) in the USCS system [30]). Also, Ahn et al. [31] reported that sandy loam is the predominant soil type for rice pad in South Korea. Additionally, our field visits indicated that the surface layer of the greenhouse ground often consists of SM or SC fill materials transported from other areas, chosen for their agricultural suitability. Based on these findings, we selected the soil types of SM and SC as the focus of our rebar stake pull-out resistance tests.

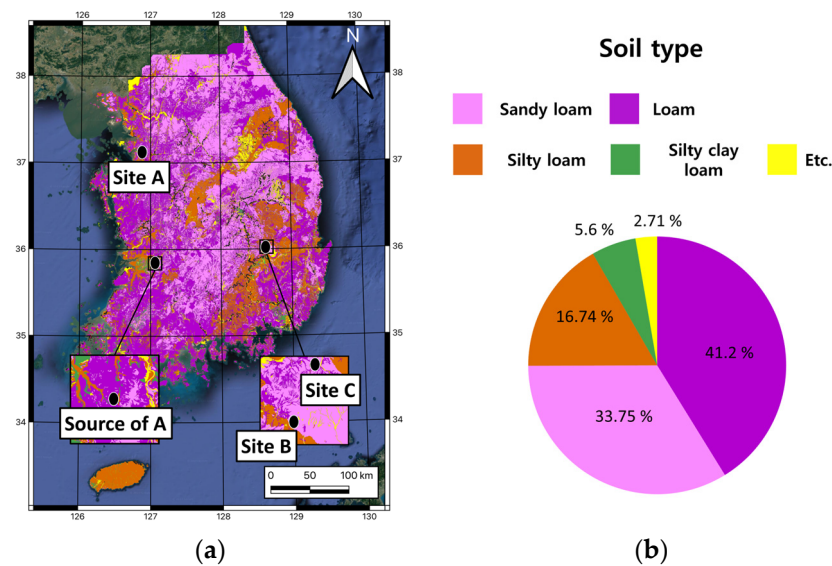


Figure 1. (a) Distribution map of surface soil type per classification in South Korea and locations of sites [32] and (b) proportion of surface soil type covering entire country.

2.2. Sites

Given that the maximum length of rebar stakes used for greenhouse reinforcement in practice does not exceed 1 m, their pull-out resistance ($R_{pull-out}$) is influenced primarily by surface soil layers no deeper than 1 m. Additionally, it is common for the surface soil beneath greenhouses to be sourced from different locations. Therefore, we established a field test site (Site A) in proximity to our laboratory for easy access (Figure 2). The site measures 2.1 m × 1.2 m with a depth of 0.5 m. The soil was sourced from a site managed by the NIAS, where actual farming was conducted as part of in situ agricultural research. According to the USCS system, the soil is classified as SM.

Site A was compacted by human weight; the soil was spreading out with a 5 cm thickness and compacted by walking back and forth on the all surface area several times. After performing field tests on this compaction condition, the surface layer was re-compacted using a hand compactor, which has a compaction force of 14.7 kN and a base plate size

of 490 mm × 360 mm, as shown in Figure 2. This mechanical compaction increased the compaction level at Site A.

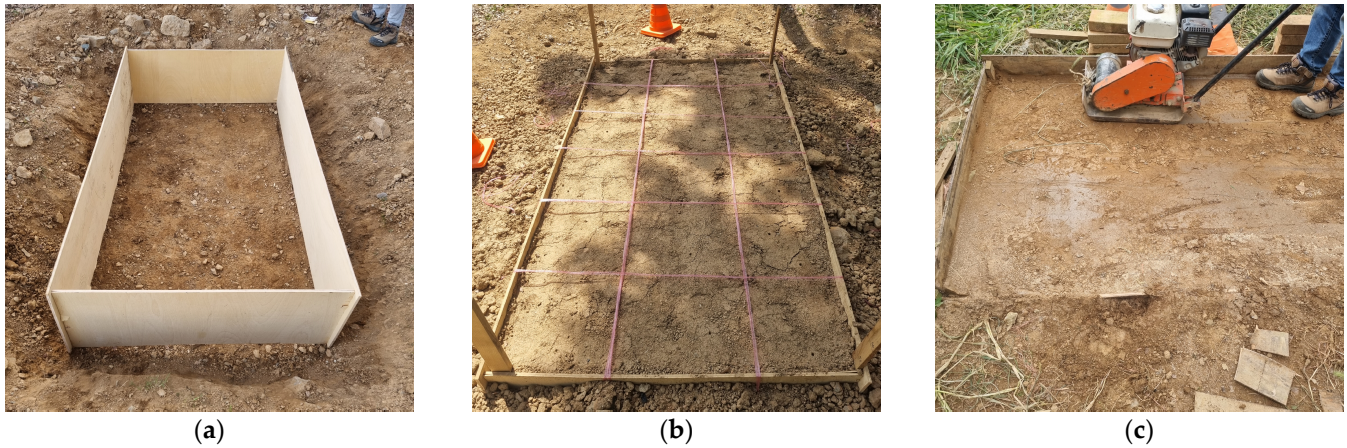


Figure 2. Site preparation process of Site A includes (a) installation of a soil box, (b) initial soil compaction using human weight, and (c) application of a hand compactor after testing under initial compaction condition.

In addition to Site A, we conducted rebar stake pull-out tests at two other field locations: Site B and Site C, where the site images are shown in Figure 3. Site B's and Site C's soil types are SC by the USCS. These sites were chosen because their soil classifications align with the most prevalent types identified in the soil condition map (as shown in Figure 1) and because they have similar soil characteristics to Site A. At Sites B and C, we carried out a series of field tests, including pull-out and cone penetration tests, along with laboratory tests on the soil samples. Figure 1a shows the locations of Sites A, B, and C, overlaying them onto the soil condition map.

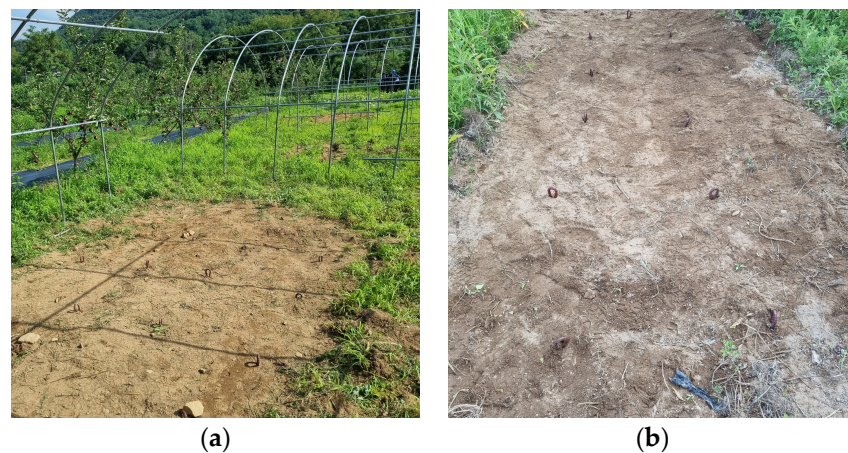


Figure 3. Field view of (a) Site B and (b) Site C.

Figure 4 shows the grain size distributions of samples from each of Sites A, B, and C, and Table 1 lists the index properties (water content, plastic limit, liquid limit, plasticity index, and soil classifications). The grain size distribution indicates the weight percent of soil passing through each sieve versus the sieve's opening size (e.g., #4 sieve has a 4.75 mm opening size), which is considered the particle diameter of soil. Site A consists of the coarsest material, and Site C is composed of the finest material among the three sites. The plastic limit (PL) and liquid limit (LL) were measured following ASTM D4318-17 [33], and the plasticity index (PI) is calculated as the difference in LL and PL. Sites A and B are classified as loam, and Site C is classified as sandy loam according to the USDA criteria, and they all conform to the SM or SC categories by the USCS.

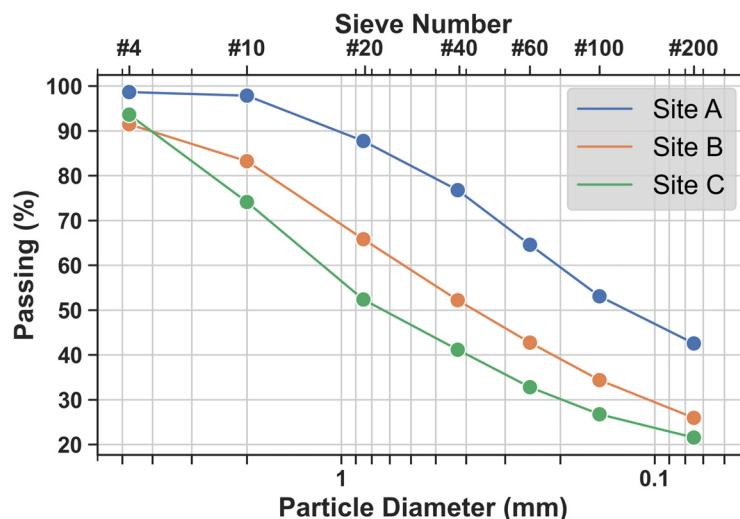


Figure 4. Grain size distributions of samples from the source site (Site A) and field test sites (Sites B and C).

Table 1. Soil properties from the source site (Site A) and field test sites (Site B and C).

Site	w (%)	PL (%)	LL (%)	PI (%)	USDA	USCS
Site A	-	27	35	8	Loam	SM
Site B	12.8–14.4	18	32	14	Loam	SC
Site C	8.2–13.2	14	32	18	Sandy Loam	SC

2.3. Laboratory and Field Tests

We conducted a comprehensive series of laboratory and field tests: (compaction test, soil compaction meter test, soil box test) as laboratory tests, and (cone penetration test, pull-out test) as field tests. These tests were designed to thoroughly evaluate the $R_{pull-out}$ of rebar stakes under various soil conditions and soil properties. The method of each test is described in this section.

2.3.1. Compaction Test

The level of soil compaction directly influences the $R_{pull-out}$ of rebar stakes. Higher compaction levels result in increased $R_{pull-out}$, whereas lower compaction levels lead to decreased resistance. By performing compaction tests with varying energy levels, we identified the optimal water content (w_{opt}) and maximum dry unit weights ($\gamma_{d,max}$) for specific compaction energies.

In South Korea, the compaction standard specifies five compaction types, which essentially represent two levels of energy [34]. Compaction types A and B are executed with an energy of $550 \text{ N}\cdot\text{mm}/\text{mm}^3$, while types C, D, and E use $2500 \text{ N}\cdot\text{mm}/\text{mm}^3$. However, these compaction types are designed for geotechnical applications, such as road pavement and embankment construction, and they typically apply more energy than what is suitable for agricultural purposes. Therefore, a compaction method with less energy than type A or B is needed in our study. In response, this study introduced a new compaction type, termed A_0 . This type was developed by reducing the number of layers and blows per layer from type A. By adjusting the number of blows per layer to 15 and the number of layers to 2, we were able to achieve a compaction energy of $220 \text{ N}\cdot\text{mm}/\text{mm}^3$, which is less than half of that used in type A. Table 2 presents the specifications of the compaction test for compaction types A_0 , A, and C.

Figure 5 presents the compaction curves for soil samples obtained from Sites A, B, and C, tested with compaction types of A_0 , A, and C. The similarity in soil classification across all sites—as they are all categorized as SM or SC by the USCS—results in similar trends in their compaction curves, regardless of the compaction types used. The compaction curve

of Site A (SM) is slightly lower than those of Sites B and C (SC) for compaction type A_0 , but they become similar for compaction types A and C. This uniformity in the compaction behavior of the soils from different sites reinforces the consistency of soil behavior between the SM and SC classifications. It also provides valuable insights into how such soils respond to various levels of compaction energy. The higher energy ends up with the higher $\gamma_{d,max}$ and the lower w_{opt} .

Table 2. Compaction test specification of A_0 proposed in this study and A and C types following the South Korea standard [34].

Type	Energy (N·mm/mm ³)	Hammer Weight (kg)	Drop Height (cm)	Blow per Layer	Number of Layers
A_0	220	2.5	30	15	2
A	550	2.5	30	25	3
C	2500	4.5	45	25	5

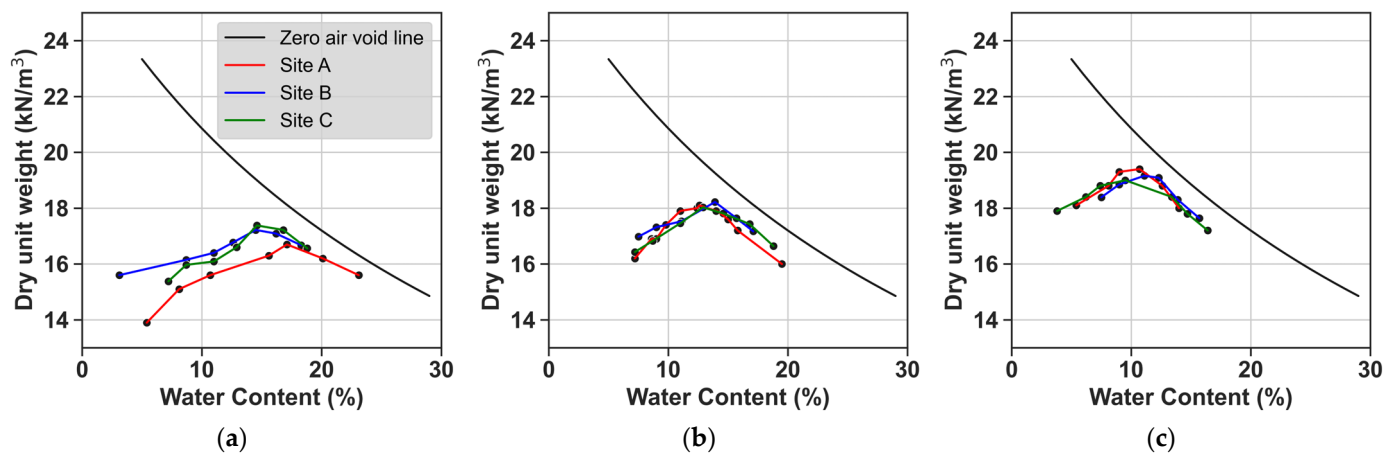


Figure 5. Compaction curves with compaction types of (a) A_0 , (b) A, and (c) C for soil samples from Sites A, B, and C.

2.3.2. Soil Compaction Meter Test

The soil compaction meter test (SCT) is employed to measure the compaction level of the surface soil. This device operates by pushing a cone into the soil surface and measuring the spring displacement (d_{sct}), which reflects the soil’s reaction stress. Figure 6 illustrates the SCT device and depicts the relationship between d_{sct} and soil reaction stress. The reaction stress increases exponentially with d_{sct} .

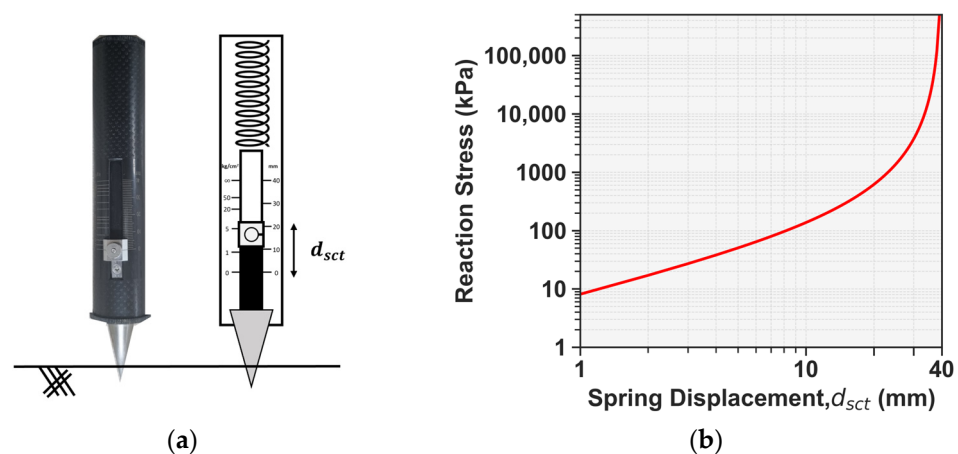


Figure 6. Soil compaction meter. (a) Photo [32]; (b) spring displacement versus soil reaction stress.

Although the SCT was originally designed to assess surface soil compaction for optimal crop growth [35,36], we adapted the SCT in our study to evaluate the compaction level by correlating it to the dry unit weight (γ_d) of the soil. The advantage of SCT is that it is easy to carry and perform, so the compaction level at the field can be easily achieved. In Figure 7, we present the results of SCT tests conducted for compacted samples of Sites A, B, and C, during three types of compaction tests (A_0 , A, and C), which are shown in Figure 5. Also, Table 3 shows the results (i.e., $\gamma_{d,max}$ and w_{opt}) of the compaction tests with types A_0 , A, and C with corresponding d_{sct} at w_{opt} ($d_{sct,opt}$). The data show a direct relationship between the $d_{sct,opt}$ and the level of compaction. The compaction type C has the greatest $d_{sct,opt}$ similar to the case of $\gamma_{d,max}$. Note that the maximum d_{sct} was shown at a water content lower than w_{opt} . This might be due to the fact that the moisture in the soil reduces the shear strength.

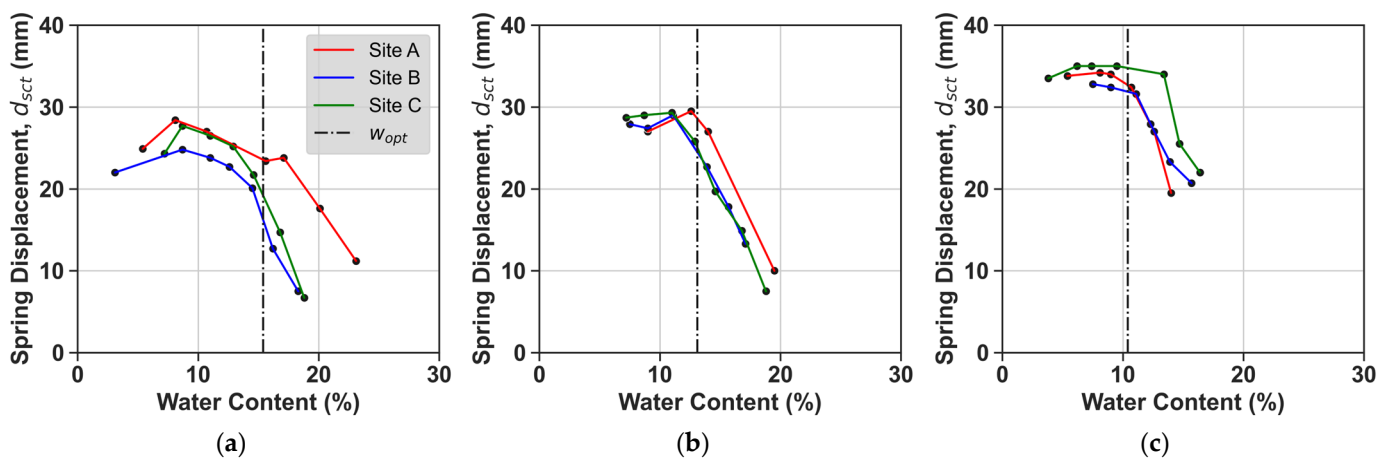


Figure 7. Spring displacement (d_{sct}) of soil compaction meter versus water content for soil samples from compaction types of (a) A_0 , (b) A, and (c) C.

Table 3. Maximum dry unit weight and spring displacement per A_0 , A, and C type compaction tests.

Type	Maximum Dry Unit Weight, $\gamma_{d,max}$ (kN/m ³)	w_{opt} (%)	Spring Displacement at w_{opt} , $d_{sct,opt}$ (mm)	Compaction Rate with Respect to Type A (%)
A_0	17.1	15.4	22	94.5
A	18.1	13.1	26	100
C	19.2	10.4	33	106.1

2.3.3. Compaction Rate

The compaction rate (CR) is an important indicator of the degree of soil compaction of the soil in the field. The CR is calculated as the ratio of γ_d to $\gamma_{d,max}$, representing the relative compaction state of soil. The γ_d refers to the unit weight of the soil measured in the field, and $\gamma_{d,max}$ represents the maximum dry unit weight that is achieved in the lab by compaction tests with a specific compaction type. In previous studies, the CR was used to represent the compaction level of soil [10,14,24–27]. Those studies commonly used compaction type A to estimate $\gamma_{d,max}$ and decide the CR.

For the estimation of γ_d and eventually CR, field tests like the sand cone and balloon tests can be used. However, they are less practical for small areas and require time for the measurement of the volume of soil and moisture evaporation. In our study, we aimed to simplify this process by establishing a correlation model between γ_d and d_{sct} . By conducting multiple compaction tests with varying energies (types A_0 , A, and C), we measured d_{sct} alongside γ_d and water content (w_c), as demonstrated in Figures 5 and 7. These results indicated a relationship between γ_d , d_{sct} , and w_c , suggesting that γ_d could be effectively

modeled using d_{sct} and w_c . The correlation model between γ_d , d_{sct} , and w_c is presented in the results section.

2.3.4. Soil Box

A soil box, sized at 400 mm × 400 mm with a depth of 800 mm, was used for pull-out tests. This box allows uniform soil compaction with controlled soil conditions. Figure 8 shows photos of the rammer, which was used to compact soil, and the soil box. We compacted soil from Sites B and C within the soil box with different compaction energies and performed rebar stake pull-out tests. The compaction method is as follows:

- Rammer size: 200 mm × 200 mm;
- Rammer weight: 95 N;
- Drop height: 1190 mm;
- Layer thickness: 2.5 cm to 5 cm;
- Total soil height: 70 cm;
- Number of blows: 1, 5, 10, and 15 per section (total 4 sections).

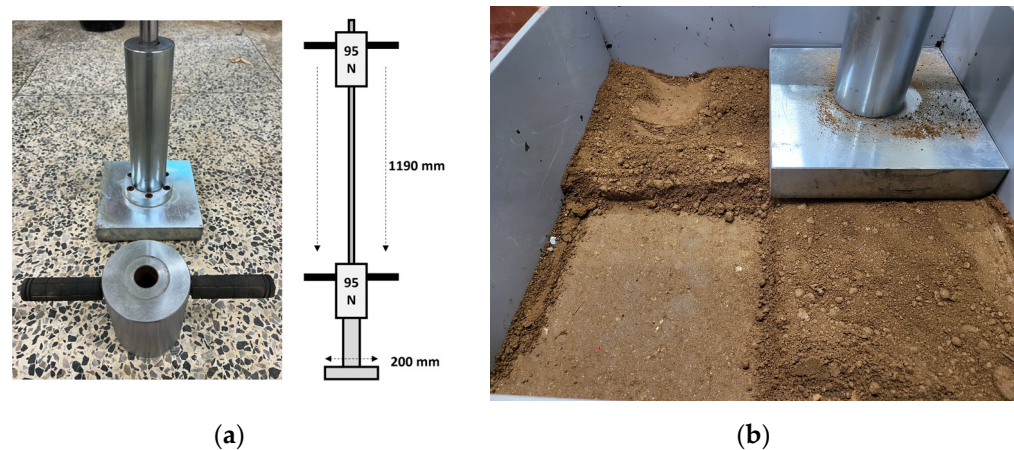


Figure 8. Photos of soil box test: (a) compaction rammer [32] and (b) soil box.

The compaction energy was controlled by the number of blows. After compaction, rebar stakes were vertically installed at 20 cm and 40 cm depths, and pull-out tests were performed.

2.3.5. Rebar Stake Pull-Out Test

The rebar stake pull-out test (RPT) involves applying a strain-controlled pull-out force to a rebar stake and measuring the force increment until the stake is extracted from the soil. This direct measurement of pull-out force provides the essential data for our analysis of rebar stake $R_{pull-out}$.

The RPT procedure is as follows:

1. Install a rebar stake into the soil at a predetermined embedded length;
2. After certain periods, apply a pull-out force to extract the stake with recording the force throughout the process.

Figure 9 shows a photograph of the RPT in action, along with a graph showing the relationship between the pull-out force and displacement. This test was conducted on Sites A, B, and C, as well as on the soil box.

2.3.6. Cone Penetration Test

The cone penetration test (CPT) is a method used to measure the resistance of soil against the penetration of a cone-shaped device [37]. This test offers valuable insights into the soil's compactness and variation continuously. For our study, we repurposed the device used for the RPT by modifying it to exert force on the soil, as depicted in Figure 10. The

device features a cone with a tip diameter of 25 mm (area = 491 mm²), which is pushed into the soil using a motor. A load cell (maximum capacity = 5000 N) is attached at the top of the rod to measure the tip resistance (q_c). Although the sleeve friction was not measured, the larger diameter of the cone compared to the rod (rod diameter = 16 mm) and the relatively shallow penetration depth (less than 200 mm) suggest that the sleeve friction does not affect q_c . The device is sufficiently weighted to enable penetration up to 1833 kPa reaction force.

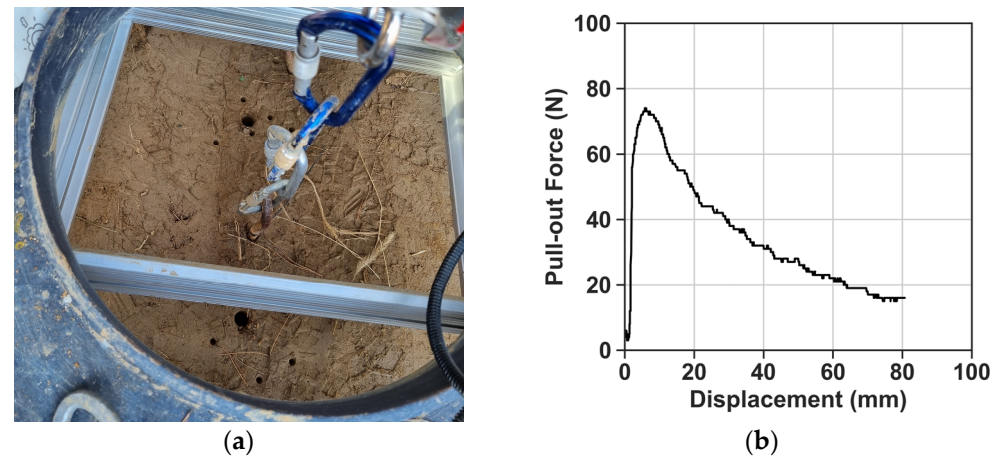


Figure 9. Rebar stake pull-out test. (a) Photo; (b) example of the measurement of pull-out force versus pull-out displacement.

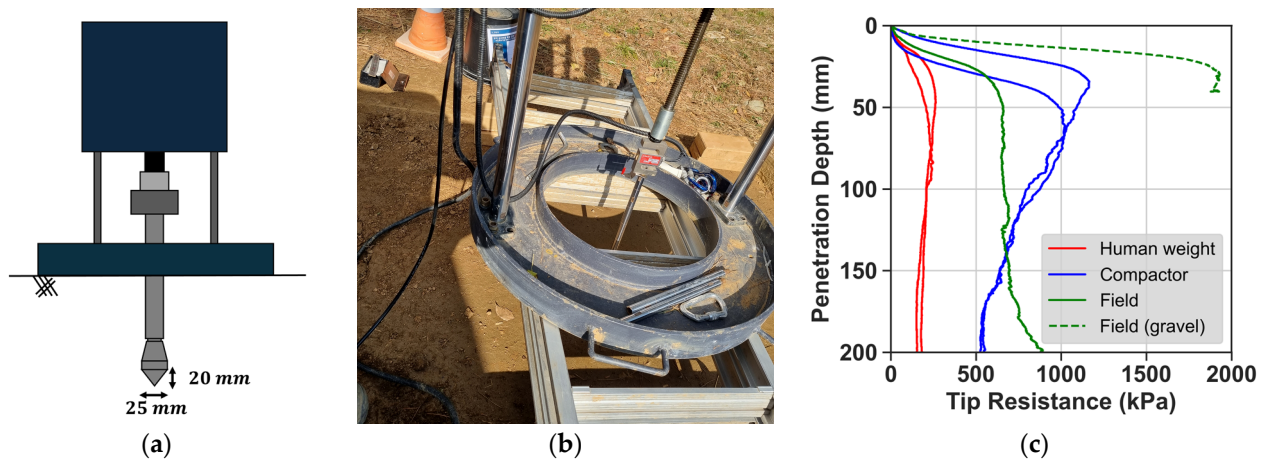


Figure 10. (a) Schematic drawing and (b) photo of portable cone penetrometer developed in this study. (c) Tip resistances at Site A with varying field compaction levels (human weight and compactor) and at Site B (field).

Figure 10c shows the relationship between q_c and penetration depth under varying soil conditions. For Site A, the q_c increases with depth if no surface compaction is applied, while the maximum q_c value occurs at a depth of 5 cm when the surface soil is compacted using the hand compactor. Nonetheless, soil with surface compaction is associated with increased q_c . However, at Site B, a natural field, we noted that q_c values were consistent in the range of 40 to 150 mm, beyond which an increasing trend was observed. From 40 to 140 mm depth, q_c at Site B was lower than at Site A with the compacted condition using a compactor. However, at depths greater than 140 mm, Site B exhibited higher q_c values. Note that in a particular test at Site B, we encountered a scenario where the cone could not penetrate beyond 40 mm and the q_c reached as high as 2000 kPa. This unusually high resistance is indicative of significant subsurface heterogeneity, potentially due to the presence of gravel. This suggests that gravel within the soil can significantly influence penetration resistance, leading to higher q_c values and measurement challenges.

3. Results

This section describes the results of the laboratory and field experiments. We first evaluated the correlation between d_{sct} and compaction level and then evaluated the ultimate $R_{pull-out}$ with respect to the compaction rate, rebar stake embedment depth, installation angle, and time.

3.1. Correlation Model for CR

The data shown in Figures 5 and 7 indicate γ_d , d_{sct} , and w_c from the same compaction test. These data were utilized to develop the correlation model, as displayed in Figure 11. For the development of a regression function, we performed two-stage regressions: (1) we first fit a linear function to the subset of data with a narrow range of w_c with respect to d_{sct} , and (2) using the functional form of the logistic regression, the slope coefficient of the first regression is fitted with respect to the median w_c at each subset. The resulting function regressed is as follows:

$$\gamma_d = \left(\frac{0.17}{1 + \exp(w_c - 11.5)^{0.78}} + 0.11 \right) \times (d_{sct} - 40) + 20 \tag{1}$$

where d_{sct} is measured in mm, w_c in %, and γ_d in kN/m^3 . The MSE of the regression is 0.288. With Equation (1), γ_d —and thus CR (equal to $\gamma_d/\gamma_{d,max}$)—can be computed if d_{sct} and w_c are known. This correlation provides a straightforward method to access CR, as SCT execution is simple: pushing a cone into the soil and measuring d_{sct} . This model enables efficiently determining soil compaction levels, which is vital for predicting the $R_{pull-out}$ of rebar stakes in various soil conditions.

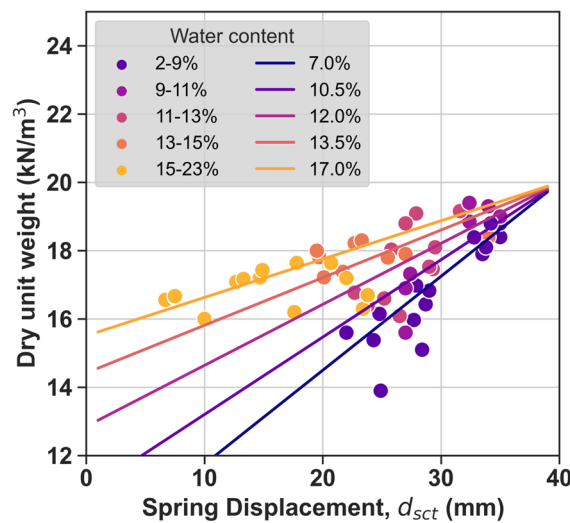


Figure 11. Relationship of dry unit weight to spring displacement dependent on water content. Correlation models are shown as solid lines.

While our correlation model (Equation (1)) effectively relates d_{sct} to CR, it is important to note that its applicability is constrained to very shallow depths, limited to a maximum penetration depth of 40 mm by the SCT. This limitation becomes critical when considering that CR can vary significantly with depth, and measuring d_{sct} at the surface may not accurately represent the CR at effective depths for estimating $R_{pull-out}$. Figure 12 presents the variation of q_c from CPT, d_{sct} , and w_c at varying depths for Site A under compactor compaction conditions. By excavating soil at 5 cm intervals, we measured d_{sct} at each depth and took soil samples for w_c measurements. The results from different days illustrate how surface w_c changes due to weather conditions, impacting d_{sct} readings. On Day 1, four days after rainfall, the surface w_c was high, leading to lower d_{sct} values. Conversely, on Day 3, seven days after rainfall, as the surface dried, w_c decreased and d_{sct} increased. Note that

the total amount of precipitation on the rainy day was 14.5 mm, and after that day, the weather condition was dried (sunny days). However, at a depth of 200 mm, the w_c and the d_{sct} values remained relatively constant across the different days. These observations indicate a crucial point; the embedment depth for greenhouse foundation reinforcement using rebar stakes is typically at least 40 cm. Hence, surface d_{sct} measurements, which can vary significantly with surface water content, may not provide a reliable indicator for estimating $R_{pull-out}$ at deeper, more relevant depths. The q_c profiles corroborate this, showing convergence at around 20 cm depth despite variations at shallower depths.

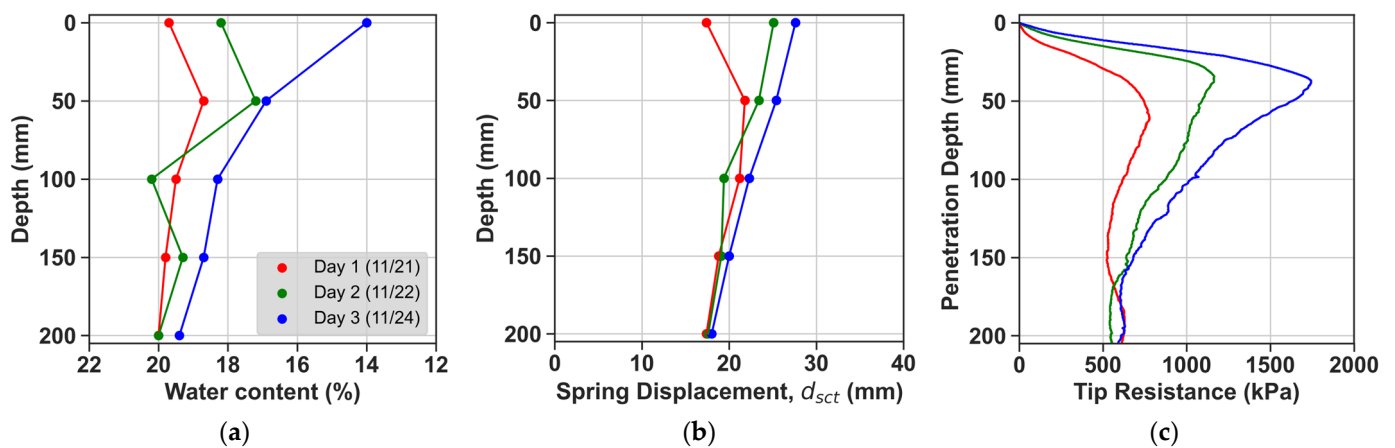


Figure 12. (a) Water content, (b) spring displacement of soil compaction meter, and (c) tip resistance of cone penetration test, showing the variations at each depth according to climatic changes at Site A.

3.2. Ultimate Pull-Out Resistance of Rebar Stake

3.2.1. Effect of Compaction Rate

We investigated the effect of CR on the $R_{pull-out}$ of rebar stakes using a soil box uniformly compacted from bottom to top. The soil box underwent five distinct levels of compaction, achieved by applying 1, 5, 10, and 15 hammer drops per layer, as illustrated in Figure 8. For each level of soil preparation, we performed the SCT to measure d_{sct} and w_c . Table 4 presents the observed d_{sct} , w_c , the derived CR using Equation (1), and the corresponding $R_{pull-out}$ of rebar stakes. We used rebar stakes with vertically embedded lengths of 20 cm and 40 cm and conducted RPTs on the same day.

Table 4. Pull-out resistances with different compaction levels using soil box tests.

Embedded Length (cm)	Hammer Drops	d_{sct} (mm)	w_c (%)	Compaction Rate (%)	Pull-Out Resistance (N)
20	1	9.9	3	64	53
	5	18.2	4.8	77	112
	10	23	4.3	84	289
	15	28.8	7.5	94	340
40	1	7	3	60	100
	5	19.1	4.7	78	359
	10	25	4.1	87	373
	15	29.3	8	95	1084

Figure 13 shows the ultimate $R_{pull-out}$ for rebar stakes at two different embedded lengths (20 cm and 40 cm), analyzed in relation to varying CRs. The data reveal a direct correlation between the increase in $R_{pull-out}$, CR, and embedded length. At a length of 20 cm, $R_{pull-out}$ exhibited a linear increase with CR. However, for stakes with an embedded length of 40 cm, the increment ratio was higher compared to the 20 cm (except for CR between 80 and 90%), resulting in $R_{pull-out}$ values exceeding 1000 N for CRs ranging from 90 to 100%. The significant disparity in $R_{pull-out}$ between the two embedded lengths, with increases

varying from 129% to 319% at each CR level, suggests varying levels of soil-stake adherence. Lower increments from 20 cm to 40 cm (e.g., 80–90% CR) imply a weaker adherence and hence only a minimal improvement in resistance. In contrast, the higher increases observed at 40 cm (e.g., 90–100% CR) indicate stronger adherence between the stake and the soil, suggesting that the stakes are more effectively anchored. This observation implies that additional measures, such as enhanced compaction after installation or tailored soil moisture management, could significantly augment the $R_{pull-out}$ of rebar stakes.

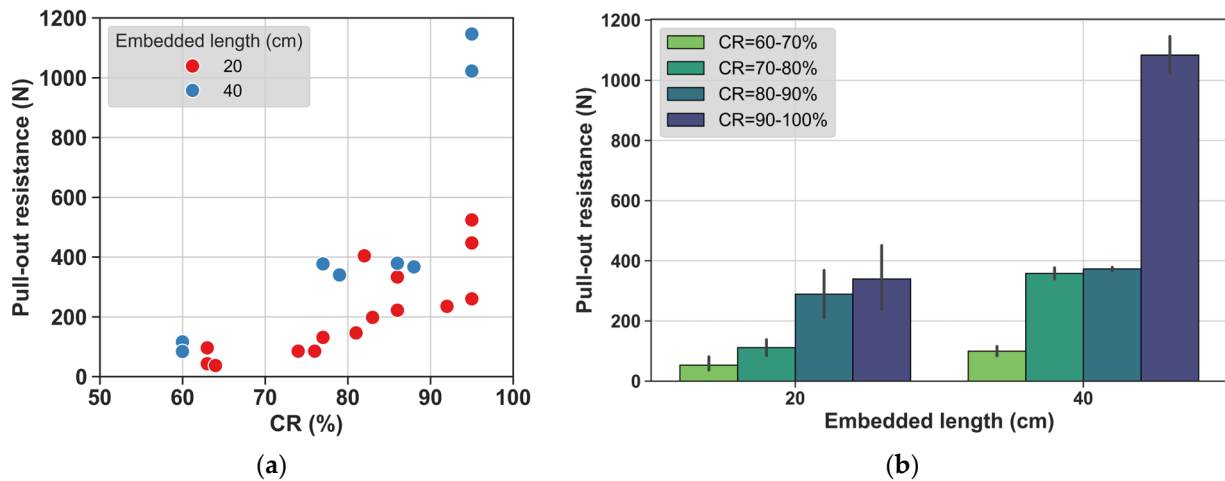


Figure 13. Ultimate pull-out resistance of rebar stakes with varying compaction rates and embedded lengths. (a) Scatter plot for pull-out resistance versus compaction rate and (b) bar chart for pull-out resistance versus embedded length.

3.2.2. Effect of Time

The $R_{pull-out}$ of rebar stakes is significantly influenced by the bond between the stake surface and the surrounding soil, which develops over time. Post-installation, gaps may initially exist between the stake and the soil. However, repeated cycles of soil wetting and drying, often occurring due to weather changes, tighten this bond, leading to an increase in $R_{pull-out}$. Figure 14 illustrates how $R_{pull-out}$ varies over time under different compaction levels: human weight and mechanical compactor at Site A.

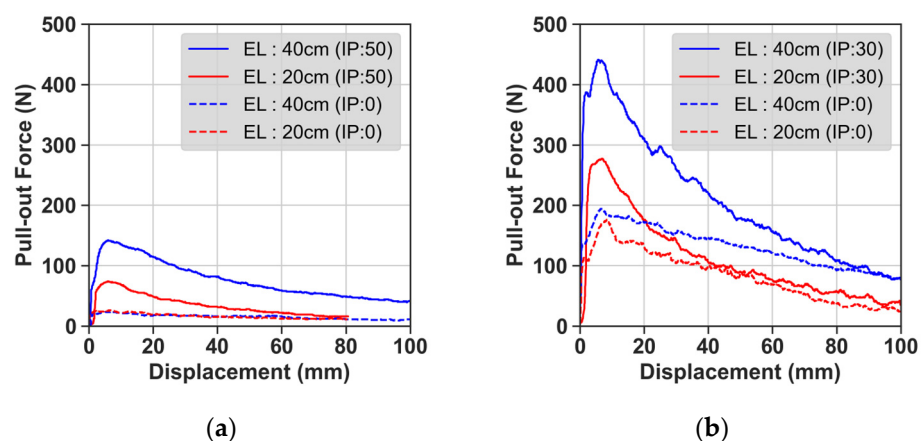


Figure 14. Pull-out resistance with different installation period (IP) and embedment depth (ED) at Site A by different compaction levels: (a) human weight and (b) compactor.

Human Weight Compaction. The immediate $R_{pull-out}$, measured on the installation day, showed minimal difference between 20 cm ($R_{pull-out} = 21$ N) and 40 cm ($R_{pull-out} = 24$ N) embedded lengths. However, stakes installed 50 days prior exhibited a substantial increase in $R_{pull-out}$ —72 N at 20 cm and 154 N at 40 cm lengths. This trend suggests an approximate

3.4-fold increase for 20 cm and a 6.4-fold increase for 40 cm compared to the initial test. The more significant increment at longer embedded length indicates that over time, the adherence between the rebar stake and soil fully develops.

Mechanical Compactor Compaction. For mechanically compacted sites, the immediate $R_{pull-out}$ values were 176 N for 20 cm and 194 N for 40 cm depths. Stakes installed 30 days earlier showed increases to 277 N (20 cm) and 441 N (40 cm), corresponding to 1.5 and 2.3 times increases, respectively. Though these increments are lower than those observed with human weight compaction, the pattern of higher increases at greater lengths remains consistent.

These observations indicate the importance of early installation of rebar stakes for achieving enhanced $R_{pull-out}$. The longer the stakes are installed, the more pronounced the resistance becomes. This finding has significant implications for optimizing the installation timing of rebar stakes, suggesting that earlier installation and longer stakes can lead to stronger soil-stake adherence and improved $R_{pull-out}$.

3.2.3. Effect of Water Content

This section examines how variations in surface w_c influence the $R_{pull-out}$ of rebar stakes in field conditions. As established in Section 3.2.1, water within the soil tends to reduce soil cohesion and decrease its density, subsequently leading to a reduction in $R_{pull-out}$.

Figure 15 illustrates the relationship between fluctuations in w_c and $R_{pull-out}$ at embedded lengths of 20 cm and 40 cm across different sites. At Site A, under human weight compaction conditions, we observed that an increase in w_c from 8.8% to 16.4% over 30 to 50 days, typically due to rainfall, significantly decreased $R_{pull-out}$. For stakes with an embedded length of 20 cm, the resistance dropped from 221 N to 72 N (a 67% reduction), and 40 cm length, from 273 N to 154 N (44% reduction). Conversely, at Sites B and C, which are naturally compacted, a decrease in w_c from 14.4% to 8.2% over 30 to 90 days, attributed to drier weather, resulted in an increase in $R_{pull-out}$. The average $R_{pull-out}$ for stakes of 20 cm embedded length increased from 160 N to 654 N (308% increase), and at 40 cm length, it increased from 242 N to 602 N (149% increase).

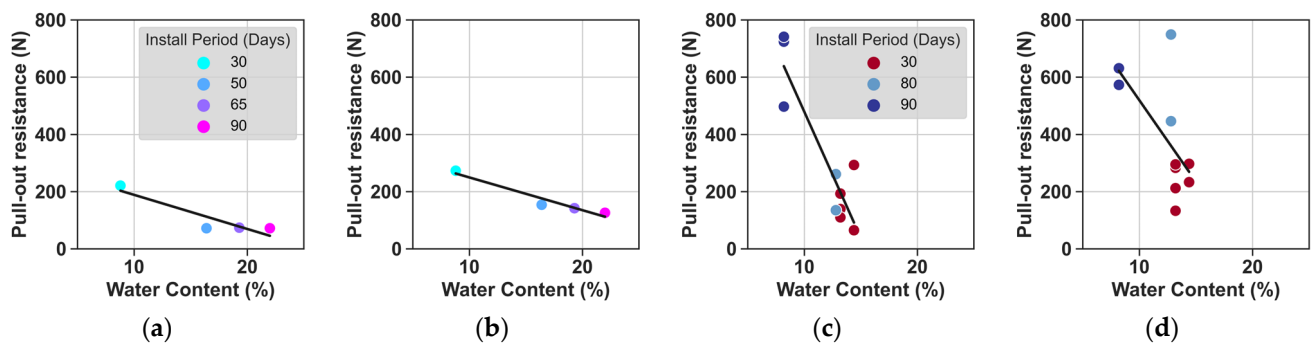


Figure 15. Ultimate pull-out resistance of rebar stakes with different embedded lengths versus variation of water contents over time. Site A with human weight compaction, (a) 20 cm depth, and (b) 40 cm depth. Sites B and C with natural compaction, (c) 20 cm depth, and (d) 40 cm depth.

These findings demonstrate that $R_{pull-out}$ is highly sensitive to changes in surface soil w_c , particularly at shallower embedded lengths. The inconsistencies, such as higher resistance at 20 cm than 40 cm, might arise due to the uncertainties inherent in field testing. During typhoon conditions, which typically bring heavy rainfall, the surface w_c can be increased significantly. Combining these observations with the results from Figure 12, it is evident that in wet conditions, longer rebar stakes are essential for maintaining adequate $R_{pull-out}$. This is because the increase in w_c at deeper depths is minimal, allowing for higher shear strength in the deeper soil layers, which in turn secures the $R_{pull-out}$.

3.2.4. Effect of Inclination Angle

In this section, we assess the impact of installation and pull-out inclination angles (α and β) on the $R_{pull-out}$ of rebar stakes. The tests, conducted at Site A with soil surface compacted using a compactor and stakes with embedded length of 40 cm, evaluated different installation angles (α : 0° , 20° , 40°) and pull-out directions (β : 0° , 10°), as depicted in Figure 16a. Figure 16b provides a typical greenhouse setup with stakes installed vertically ($\alpha = 0^\circ$) and inclined towards the greenhouse walls ($\beta > 0^\circ$).

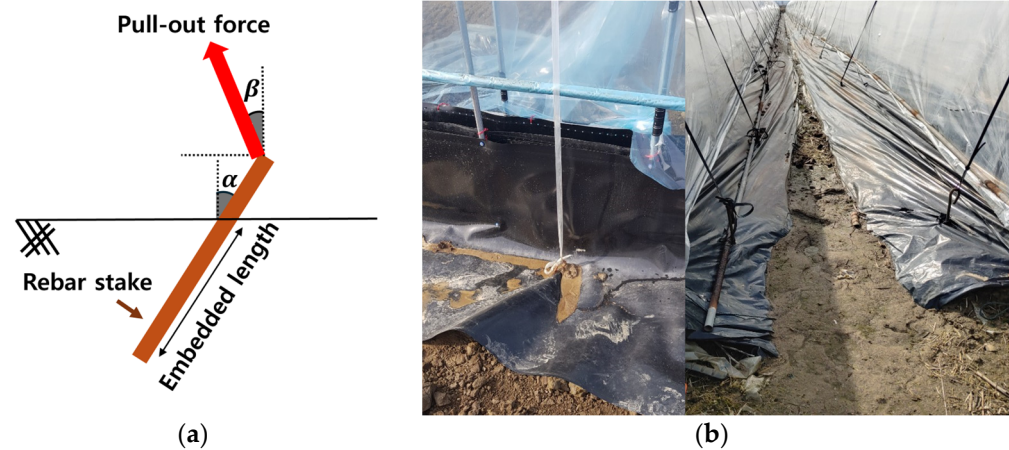


Figure 16. (a) Description of inclination angles of installation (α) and pull-out direction (β) and (b) photos of field installation conditions.

The RPTs were conducted at Site A with a consistent 40 cm embedded length on different days. Figure 17 shows variation in d_{sct} and w_c at each depth. The d_{sct} ranged from 20 to 30 mm on Day 1 and 20 to 26 mm on Day 2, with w_c between 10 and 21% and 14 and 19%, respectively, where surface w_c at Day 1 was 10% and 14% at Day 2. Despite an increase in surface w_c due to rain between those days, the deeper layers (e.g., 20 cm) showed minimal variation in d_{sct} and w_c , maintaining an average CR above 95% in the range of 0 to 20 cm depth. Comparing Day 1 and Day 2, Day 1, with a lower w_c at surface, has a higher $R_{pull-out}$ than one of Day 2 (Day 1: solid lines; Day 2: dotted lines in Figure 18).

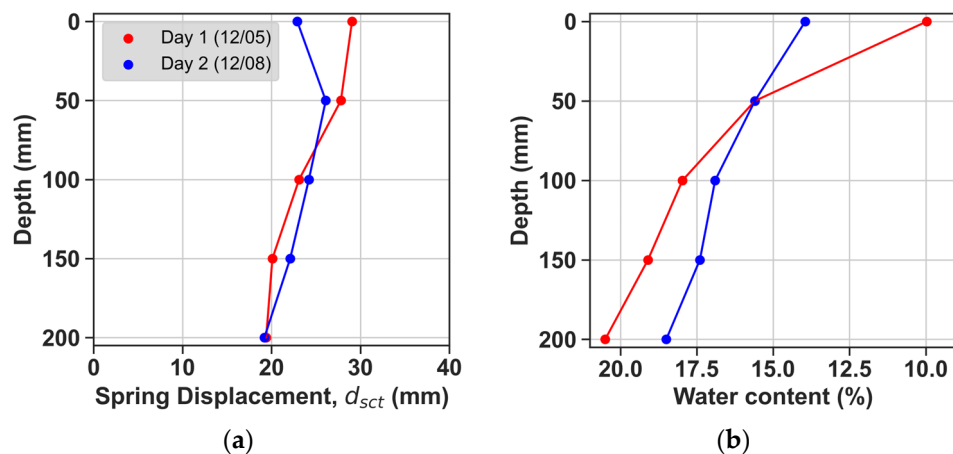


Figure 17. Variation in (a) spring displacement and (b) water content at Site A.

Figure 18 presents the pull-out forces against displacements for each angle combination. The variation of $R_{pull-out}$ is greater with changes in α and β than changes in w_c . With α at 0° , the average $R_{pull-out}$ was 196 N for $\beta = 0^\circ$ and 350 N for $\beta = 10^\circ$. Increasing α to 20° resulted in average resistances of 653 N ($\beta = 0^\circ$) and 962 N ($\beta = 10^\circ$), indicating a substantial effect of the installation angle on resistance, with increases ranging from 2.5 to 3.5-fold compared to $\alpha = 0^\circ$. For α at 40° , with β at both 0° and 10° , the measured values

were 847 N and 856 N, respectively, higher than $\alpha = 0^\circ$ but similar to $\alpha = 20^\circ$ cases. For $\alpha = 20^\circ$ and 40° cases, the increase in β from 0° to 10° did not significantly alter $R_{pull-out}$.

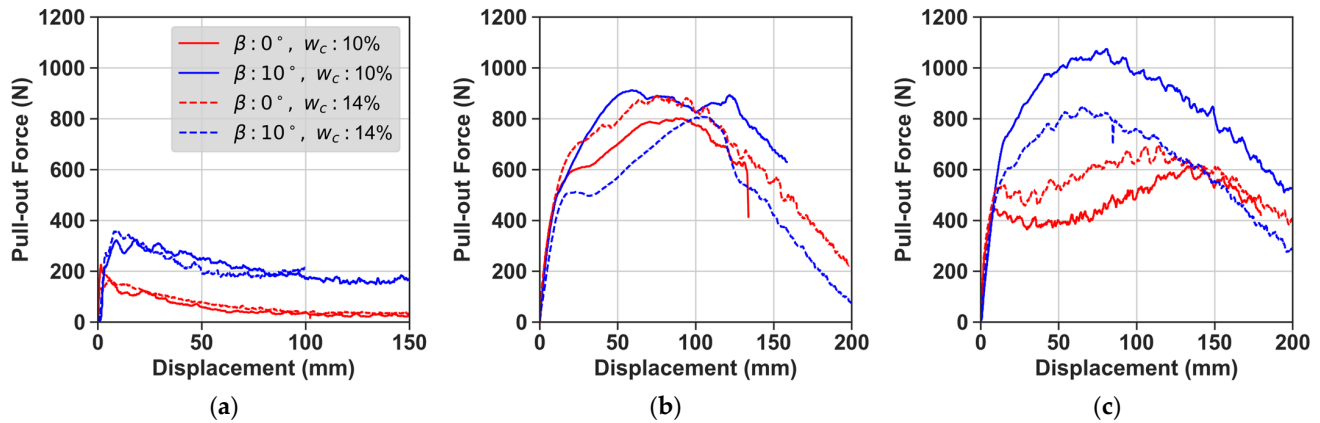


Figure 18. Pull-out forces versus displacements with different installation inclinations angles (α): (a) 0 degree, (b) 20 degrees, and (c) 40 degrees with 0 and 10 degrees of pull-out direction inclination angles (β).

These increases in $R_{pull-out}$ for inclined installations can be attributed to the additional mechanism where the stake pushes against the soil, triggering passive soil failure. This phenomenon significantly enhances $R_{pull-out}$. Also, during our tests, we observed ductile fractures in rebar stakes under inclined conditions. Ductile fractures provide a form of safety prior to complete failure, allowing for early detection and preventive measures in greenhouse structures.

4. Discussion

4.1. Suggestion of Rebar Stake Installation

Based on our analysis of factors influencing rebar stake $R_{pull-out}$, we propose the following guidelines for their optimal installation, particularly in greenhouse environments.

Compaction Level. Our findings demonstrate the significant role of soil compaction level in enhancing $R_{pull-out}$. $R_{pull-out}$ at a CR of 90–100% relative to type A compaction (with $\gamma_{d,max}$ of 18.1 kN/m^3) was observed to be ten times higher than at 60–70% CR, particularly for rebar stakes with an embedded length of 40 cm. This increase highlights the importance of achieving a high CR for maximized $R_{pull-out}$. Additionally, surface compaction using mechanical compactors proved to be beneficial in forming a densely compacted soil layer approximately 5 cm deep. This compacted layer effectively reduces water infiltration into deeper layers [38], which is advantageous in minimizing the loss of $R_{pull-out}$ during conditions of heavy rain. Given these observations, we recommend assessing d_{sct} at a minimum depth of 5 cm, not surface. This is crucial because surface d_{sct} readings can be highly variable due to weather conditions, whereas $R_{pull-out}$ is more reliant on the compaction at deeper depths. If d_{sct} readings exceed 20 mm at depth in wet conditions ($w_c > 16\%$), it can be inferred that the CR is above 90%, which we identify as the recommended condition for securing optimal $R_{pull-out}$.

Embedded Length. The $R_{pull-out}$ with 40 cm embedded length has 2 to 3 folds of $R_{pull-out}$ compared to the 20 cm embedded length in the case of vertical installation. Based on these findings, we recommend an embedded length of greater than 40 cm for rebar stakes. This recommendation is particularly pertinent considering heavy rainfall. During rainfall, the surface soil tends to become saturated, leading to a reduction in shear strength. However, for rebar stakes with greater embedded length, the impact of surface wetness is mitigated. As stated above, the filtration of water into the soil is reduced in deeper, especially compacted, soil layers. As a result, the reduction in $R_{pull-out}$ due to rain conditions is limited. Therefore, a minimum embedded length of 40 cm not only enhances the $R_{pull-out}$ under normal conditions but also ensures reliability and effectiveness during heavy rainfall.

Inclination Angles. The installation angle (α) and the angle of pull-out direction (β) greatly affect the $R_{pull-out}$. Rebar stakes installed with $\alpha = 20^\circ$ have 2.5 to 3.5 folds higher $R_{pull-out}$ compared to the $\alpha = 0^\circ$ case, and the change in $\beta = 0^\circ$ to 10° increases $R_{pull-out}$ by 150% at $\alpha = 0^\circ$ case. We suggest an α of approximately 20° and a $\beta > 0^\circ$. This configuration has been shown to maximize $R_{pull-out}$ where the passive soil failure mechanism provides enhanced resistance.

Installation Time. Our findings indicate an increase in $R_{pull-out}$ when there is sufficient time for the soil to bond with the rebar stake surface through wetting and drying cycles. Compared to immediate $R_{pull-out}$, the increment ratio of post-installation is in the range of 150% to 640%, depending on the embedded length and compaction level, where $R_{pull-out}$ increased in all cases. Therefore, we advise installing rebar stakes at least one month before the strong wind season to take advantage of this bonding process.

4.2. Comparison of Pull-Out Resistance with Other Foundation Types

In this section, we compare the $R_{pull-out}$ of rebar stakes to that of other foundation types, including rafter pipe, spiral steel peg, spiral bar, and continuous pipe foundations, as evaluated in previous studies [10,14,24,25]. Each foundation type is visually shown in Figure 19.

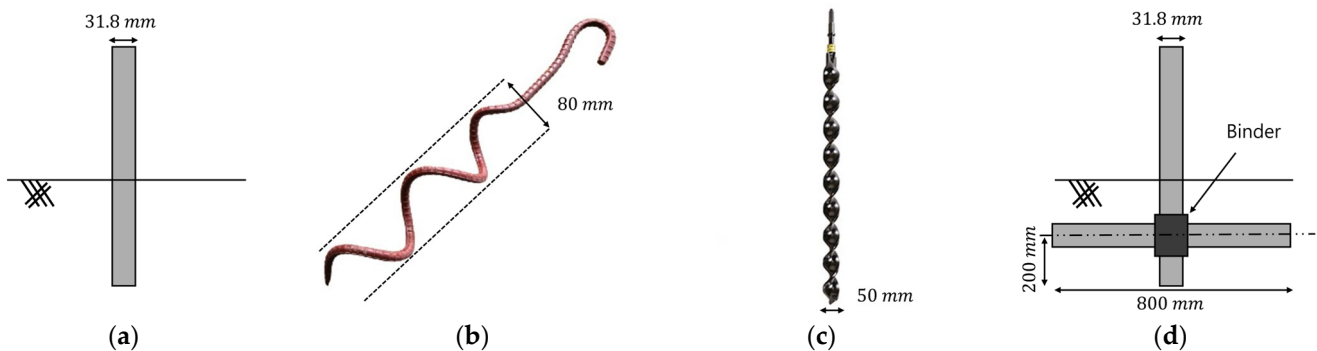


Figure 19. Examples of (a) rafter pipe, (b) spiral steel peg, (c) spiral bar, and (d) continuous pipe foundation.

Figure 20a presents the $R_{pull-out}$ of rebar stakes from this study at different installation angles (refer to Figure 18) alongside the $R_{pull-out}$ of rafter pipe, spiral steel peg, and spiral bar from previous studies [10,14,25], which used sandy loam in soil box experiments. The embedded lengths in all other studies were consistent at 40 cm, and the installation and pull-out directions were vertical. Previous studies conducted similar experiments in sandy loam within a soil box measuring 800 mm \times 1000 mm \times 600 mm with 65, 75, and 85% CR. The w_c used was w_{opt} (=16.2%) at compaction, and they tested $R_{pull-out}$ on the same day of installation. At an 85% CR, the $R_{pull-out}$ of rafter pipes (diameter of 31.8 mm) was higher at 521 N compared to the vertical $R_{pull-out}$ of rebar stakes (diameter of 13 mm), which was 226 N. However, when rebar stakes were installed at an angle (α) of 20° or more, their resistance increased to 962 N (Figure 18b). This indicates that the installation angle enhances the efficacy of rebar stakes. The $R_{pull-out}$ for spiral steel pegs was found to be 1144 N, which is similar to the inclined rebar stake. The spiral bar, with a diameter of 50 mm, exhibited a significantly higher $R_{pull-out}$ of 3359 N, about three times that of the rebar stake.

A further comparison was made with continuous pipe foundations composed of rafter pipes and crossbars (illustrated in Figure 19d), based on previous studies [24,25]. Similarly, these studies used w_c in a range of 16.2% to 16.6%, and the immediate $R_{pull-out}$ values were measured. Variations in $R_{pull-out}$ were observed depending on the binder and compaction rate (Figure 20b). The steel wire binder at a 50 cm embedment depth yielded an $R_{pull-out}$ of only 186 N, likely due to binder slippage before soil failure. Conversely, stronger binders against slippage like steel plates and U-clamps significantly increased the $R_{pull-out}$, with the

U-clamp method at a 40 cm embedment depth reaching an $R_{pull-out}$ of 2953 N. This $R_{pull-out}$ is also about three times that of rebar stakes.

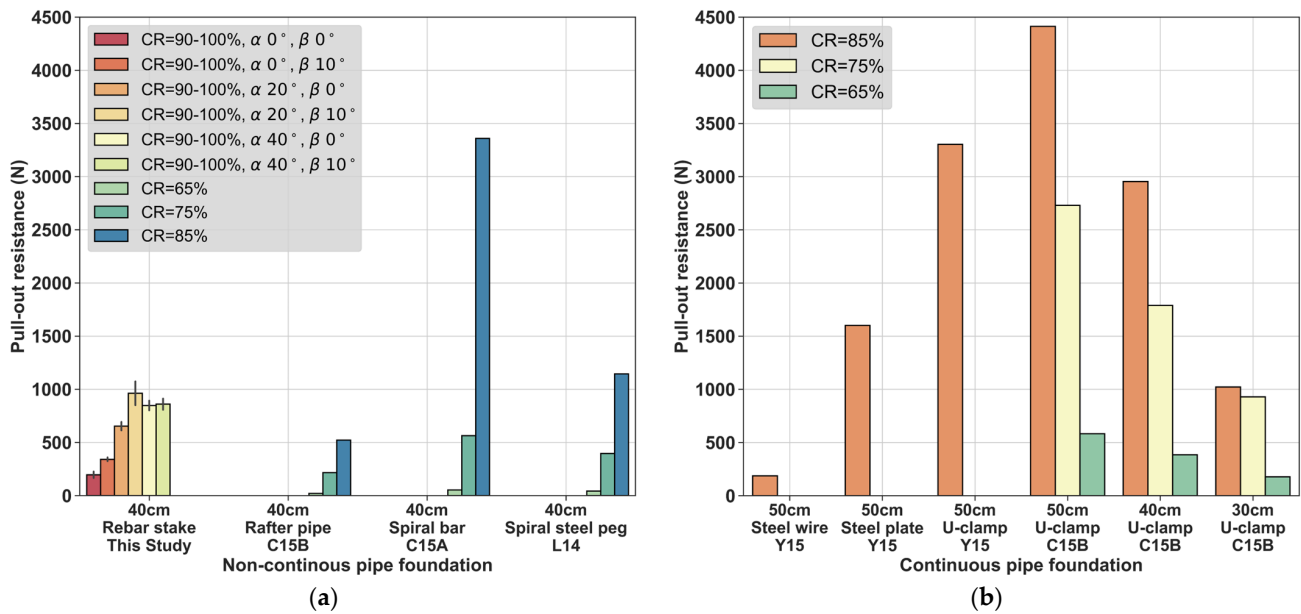


Figure 20. Comparison of pull-out resistance among (a) non-continuous pipe foundations and (b) continuous pipe foundations among this study and previous studies (Choi et al. [10] as C15A, Choi et al. [25] as C15B, Lee et al. [14] as L14, and Yun et al. [24] as Y15).

Table 5 summarizes the $R_{pull-out}$ values for each foundation type from the various studies and this study. This comparative analysis highlights that continuous pipe foundations, as recommended by disaster-resistant criteria, offer higher $R_{pull-out}$ values at the same embedment depth than other foundation types. Similarly, the spiral bar is also effective against uplift forces. If at least three rebar stakes were installed at a horizontal length of 800 mm, the $R_{pull-out}$ would be comparable to one of a continuous pipe foundation. Note that the cost of reinforcing existing greenhouses with continuous pipe or spiral bar foundations is higher compared to installing rebar stakes.

Table 5. The $R_{pull-out}$ values for each foundation type from various studies.

Type	Reference	Foundation	w_c (%)	Compaction Rate	Pull-Out Resistance (N)		
					30 cm	40 cm	50 cm
Non-continuous pipe foundation	Choi et al. [10] (C15A)	Spiral bar	16.2	65%	-	53	-
				75%	-	563	-
				85%	-	3359	-
	Lee et al. [14] (L14)	Spiral steel peg	16.2	65%	-	43	-
				75%	-	396	-
				85%	-	1144	-
	Choi et al. [25] (C15B)	Rafter pipe	16.2	65%	-	20	-
				75%	-	216	-
				85%	-	521	-
	This study	Rebar stake	13.1	90–100%	-	196 ($\alpha = 0^\circ, \beta = 0^\circ$)	-
-					341 ($\alpha = 0^\circ, \beta = 10^\circ$)	-	
-					653 ($\alpha = 20^\circ, \beta = 0^\circ$)	-	
-					962 ($\alpha = 20^\circ, \beta = 10^\circ$)	-	
-					847 ($\alpha = 40^\circ, \beta = 0^\circ$)	-	
-					860 ($\alpha = 40^\circ, \beta = 10^\circ$)	-	

Table 5. Cont.

Type	Reference	Foundation	w_c (%)	Compaction Rate	Pull-Out Resistance (N)		
					30 cm	40 cm	50 cm
Continuous pipe foundation	Yun et al. [24] (Y15)	Steel wire	16.6	85%	-	-	186
		Steel plate		85%	-	-	1601
		U-clamp		85%	-	-	3303
	Choi et al. [25] (C15B)	U-clamp	16.2	65%	177	384	582
				75%	929	1788	2729
				85%	1022	2953	4413

5. Conclusions

This study evaluated the pull-out resistance of rebar stakes, commonly used for reinforcing the foundations of greenhouses not constructed following disaster-resistant standards. The evaluation was conducted considering various factors, such as compaction level, installation angle, time, and water content, through a combination of field and laboratory tests. The findings for enhancing the pull-out resistance of rebar stakes can be summarized as follows:

1. Both this study and previous studies indicate that soil compaction significantly impacts the pull-out resistance of greenhouse foundations. A higher compaction rate leads to increased pull-out resistance. The use of compactors to densify the surface layer of soil creates a compacted layer underneath, reducing water infiltration during heavy rainfall and minimizing the loss of pull-out resistance. Given the potential impact of soil moisture on pull-out resistance, an embedded length of at least 40 cm for rebar stakes is advised.
2. Post-installation, the pull-out resistance of rebar stakes increases over time. Weather-induced fluctuations in soil moisture content enhance the bond between the stake surface and the soil, thereby increasing the pull-out resistance. For optimal resistance, it is recommended to install rebar stakes at least a month ahead of the anticipated strong wind season.
3. This study highlights that the installation angle critically affects pull-out resistance. While vertical installations rely solely on the cohesion between the stake and soil during pull-out, inclined installations benefit from passive soil failure, increasing resistance. An installation angle (α) of 20° and a pull-out direction (β) exceeding 0° are suggested to effectively enhance the resistance.
4. Rebar stakes with a 40 cm embedded length, a compaction rate over 90%, and an α of 20° exhibited a pull-out resistance of around 1000 N. This resistance is greater than that of a single vertical rafter pipe and is similar to that of a spiral steel peg foundation. To match the performance of a 50 mm diameter spiral bar or an 800 mm length continuous pipe foundation, the installation of three appropriately positioned rebar stakes is necessary.

These conclusions highlight critical factors affecting rebar stake pull-out resistance and offer actionable guidelines for their optimal use in greenhouse foundations. The limitation of the test results in this study is that due to the heterogeneity of soil material and anisotropic field compaction level at each test location, the values of $R_{pull-out}$ at each condition would be varied. However, the suggested $R_{pull-out}$ of 1000 N with a longer than 40 cm embedded length, a compaction rate over 90%, and 20° inclination conditions is at the lower end, so it can be used as a design value. Future research directions include numerical simulations of rebar stake pull-out resistance, focusing on combination effects of factors and fine-tuning the optimal installation angle and stake length for maximum efficacy.

Author Contributions: Conceptualization, G.H., I.C., H.L., S.L. and D.K.; methodology, G.H., I.C. and D.K.; software, G.H.; validation, G.H., I.C. and J.L.; formal analysis, G.H.; investigation, G.H., I.C. and J.L.; resources, H.L. and S.L.; data curation, G.H. and I.C.; writing—original draft preparation, G.H. and D.K.; writing—review and editing, G.H., I.C., J.L., H.L., S.L. and D.K.; visualization, G.H.; supervision, D.K.; project administration, S.L.; funding acquisition, S.L. and D.K. All authors have read and agreed to the published version of the manuscript.

Funding: This research was funded by the Rural Development Administration, grant number RS-2021-RD009628, and the Basic Research Program through the National Research Foundation of Korea, grant number RS-2023-00220751.

Data Availability Statement: The data presented in this study are available on request from the corresponding author. The data are not publicly available due to privacy.

Conflicts of Interest: The authors declare no conflicts of interest. The funders had no role in the design of the study; in the collection, analyses, or interpretation of data; in the writing of the manuscript; or in the decision to publish the results.

References

1. Uematsu, Y.; Takahashi, K. Collapse and reinforcement of pipe-framed greenhouse under static wind loading. *J. Civ. Eng. Archit.* **2020**, *14*, 583–594.
2. Wang, C.; Nan, B.; Wang, T.; Bai, Y.; Li, Y. Wind pressure acting on greenhouses: A review. *Int. J. Agric. Biol. Eng.* **2021**, *14*, 1–8. [[CrossRef](#)]
3. Jung, I.W.; Bae, D.H.; Kim, G. Recent trends of mean and extreme precipitation in Korea. *Int. J. Climatol.* **2011**, *31*, 359–370. [[CrossRef](#)]
4. Kim, J.S.; Kang, H.W.; Son, C.Y.; Moon, Y.I. Spatial variations in typhoon activities and precipitation trends over the Korean Peninsula. *J. Hydro-Environ. Res.* **2016**, *13*, 144–151. [[CrossRef](#)]
5. Ha, T.; Kim, J.; Cho, B.H.; Kim, D.J.; Jung, J.E.; Shin, S.H.; Kim, H. Finite element model updating of multi-span greenhouses based on ambient vibration measurements. *Biosyst. Eng.* **2017**, *161*, 145–156. [[CrossRef](#)]
6. Yoon, Y.C.; Suh, W.M.; Yoon, C.S. A Study on the Typhoon Disaster of Greenhouse. *J. Bio-Environ. Control* **1995**, *4*, 167–174. (In Korean)
7. Rural Development Administration (RDA). *Symposium for Reducing of Meteorological Disasters of Agricultural Facilities*; RDA: Suwon, Republic of Korea, 2007; pp. 160–161. (In Korean)
8. Statistics Korea. Korean Statistical Information Service (KOSIS). Damage by Causes of Natural Disasters. 2023. Available online: https://kosis.kr/statHtml/statHtml.do?orgId=110&tblId=DT_156003_014&vw_cd=MT_ZTITLE&list_id=C_21 (accessed on 6 January 2023). (In Korean)
9. Ministry of Agriculture, Food and Rural Affairs (MAFRA). *Design and Specifications of Standardized Anti-Disaster Prototypes for Greenhouses*; Specification 2014–2078; MAFRA: Sejong, Republic of Korea, 2014. (In Korean)
10. Choi, M.K.; Yun, S.W.; Kim, H.N.; Lee, S.Y.; Kang, D.H.; Yoon, Y.C. Uplift capacity of spiral bar through the model experiment. *J. Bio-Environ. Control* **2015**, *24*, 202–209. (In Korean) [[CrossRef](#)]
11. Fernández-García, M.S.; Vidal-López, P.; Rodríguez-Robles, D.; Villar-García, J.R.; Agujetas, R. Numerical simulation of multi-span greenhouse structures. *Agriculture* **2020**, *10*, 499. [[CrossRef](#)]
12. Kim, M.H. Effects of Uplift Resistance on Continuous-Pipe-Foundation of Single-Span Plastic Greenhouse by Steel Plate Pipe Connector. *Agriculture* **2022**, *12*, 1998. [[CrossRef](#)]
13. Kim, M.H.; Song, C.M. Deep Neural Network Analysis on Uplift Resistance of Plastic Greenhouses for Sustainable Agriculture. *Sustainability* **2023**, *15*, 5632. [[CrossRef](#)]
14. Lee, B.G.; Yun, S.W.; Choi, M.K.; Lee, S.Y.; Moon, S.D.; Yu, C.; Yoon, Y.C. Uplift bearing capacity of spiral steel peg for the single span greenhouse. *J. Bio-Environ. Control* **2014**, *23*, 109–115. (In Korean) [[CrossRef](#)]
15. Lee, S.I.; Lee, J.H.; Jeong, Y.J.; Choi, W. Development of a structural analysis model for pipe structures to reflect ground conditions. *Biosyst. Eng.* **2020**, *197*, 231–244. [[CrossRef](#)]
16. Lee, W.G.; Woo, J.H.; Lee, H.D.; Shin, K.J. Analysis of Uplift Capacity on Single-span Greenhouse's Foundation According to Wind Load and Evaluation for Reinforcing Methods. *J. Reg. Assoc. Archit. Inst. Korea* **2022**, *24*, 33–39. (In Korean)
17. Pack, M.; Mehta, K. Design of affordable greenhouses for East Africa. In Proceedings of the 2012 IEEE Global Humanitarian Technology Conference, Seattle, WA, USA, 21–24 October 2012; pp. 104–110.
18. Peña, A.; Valera, D.; Pérez, F.; Ayuso, J.; Pérez, J. Behavior of greenhouse foundations subjected to uplift loads. *Trans. ASAE* **2004**, *47*, 1651–1657. [[CrossRef](#)]
19. Peña, A.A.; Martínez, D.L.V.; Alonso, J.P. Estimate of the Load Capacity to Traction of Foundations for Greenhouses. In Proceedings of the 2002 ASAE Annual Meeting, Chicago, IL, USA, 28–31 July 2002; p. 024011.
20. Tsai, M.-H.; Lee, Y.-C. Practical Structural Design and Construction of an Innovative Composite Plastic Greenhouse. *Agriculture* **2021**, *11*, 1051. [[CrossRef](#)]

21. Von Elsner, B.; Briassoulis, D.; Waaijenberg, D.; Mistriotis, A.; Von Zabeltitz, C.; Graud, J.; Russo, G.; Suay-Cortes, R. Review of structural and functional characteristics of greenhouses in European Union countries: Part I, design requirements. *J. Agric. Eng. Res.* **2000**, *75*, 1–16. [[CrossRef](#)]
22. Yun, S.W.; Choi, M.K.; Yu, C.; Lee, S.Y.; Yoon, Y.C. Analysis of Working Load based on Wind and Snow Load for Greenhouse Foundation. *J. Agric. Life Sci.* **2014**, *48*, 183–188. [[CrossRef](#)]
23. Yun, S.W.; Shin, Y.S.; Yu, C.; Yoon, Y.C. Analysis of working load on greenhouse foundation considering wind and snow load. *Acta Hortic.* **2014**, *1037*, 99–104. [[CrossRef](#)]
24. Yun, S.Y.; Choi, M.K.; Lee, Y.S.; Yoon, Y.C. Uplift Capacity of Continuous Pipe Foundation for Prevention of Meteorological Disaster. *J. Agric. Life Sci.* **2015**, *49*, 303–310. (In Korean) [[CrossRef](#)]
25. Choi, M.K.; Yun, S.W.; Kim, H.N.; Lee, S.Y.; Yu, C.; Yoon, Y.C. Uplift capacity of pipe foundation for single-span greenhouse. *J. Bio-Environ. Control* **2015**, *24*, 69–78. (In Korean) [[CrossRef](#)]
26. Lim, S.Y.; Kim, Y.Y.; Yu, S.C.; Kim, M.H. Characteristics of uplift capacity of a embedded foundation and soil type. *J. Korean Soc. Agric. Eng.* **2019**, *61*, 23–30. (In Korean)
27. Song, C.S.; Jang, U.H.; Choi, D.H.; Kim, J.C. Characteristics of uplift capacity of house pipe foundation according to foundation types and soil conditions. *J. Korean Soc. Agric. Eng.* **2020**, *62*, 117–126. (In Korean)
28. Korean Soil Information System (KSIS). Categorization of Agricultural Soil by Type in Republic of Korea, KSIS. Available online: <http://soil.rda.go.kr/geoweb/soilmain.do> (accessed on 6 January 2023). (In Korean)
29. United States Department of Agriculture (USDA). *Soil Taxonomy: A Basic System of Soil Classification for Making and Interpreting Soil Surveys*; Agriculture handbook Number 436; United States Department of Agriculture Natural Resources Conservation Service: Washington, DC, USA, 1999; 869p.
30. Casagrande, A. Classification and identification of soils. *Trans. Am. Soc. Civ. Eng.* **1948**, *113*, 901–930. [[CrossRef](#)]
31. Ahn, B.K.; Lee, J.H.; Kim, K.C.; Kim, H.G.; Jeong, S.S.; Jeon, H.-W.; Zhang, Y.-S. Changes in chemical properties of paddy field soils as influenced by regional topography in Jeonbuk Province. *Korean J. Soil Sci. Fertil.* **2012**, *45*, 393–398. (In Korean) [[CrossRef](#)]
32. Choi, I.H.; Heo, G.S.; Lee, J.Y.; Kwak, D.Y. Prediction of Pull-Out Force of Steel Pegs Using the Relationship Between Degree of Compaction and Hardness of Soil Conditioned on Water Content. *J. Korean Geotech. Soc.* **2023**, *39*, 23–35. (In Korean)
33. *ASTM D4318-17*; Standard Test Methods for Liquid Limit, Plastic Limit, and Plasticity Index of Soils. ASTM: West Conshohocken, PA, USA, 2018.
34. *KS F 2312*; Test Method for Soil Compaction in Laboratory. Korea Industrial Standards Commission: Seongnam, Republic of Korea, 2011. (In Korean)
35. de Moraes, M.T.; da Silva, V.R.; Zwirter, A.L.; Carlesso, R. Use of penetrometers in agriculture: A review. *Eng. Agrícola* **2014**, *34*, 179–193. [[CrossRef](#)]
36. Nakayama, Y. Theory and practice of a soil hardness tester YH-62. In *Penetration Testing*; Routledge: Abingdon, UK, 2021; Volume 1, pp. 303–308.
37. *KS F 2592*; Standard Test Method for Electronic Cone Penetration of Soils. Korea Industrial Standards Commission: Seongnam, Republic of Korea, 2014. (In Korean)
38. Tekeste, M.Z.; Raper, R.L.; Schwab, E.B. Soil drying effects on soil strength and depth of hardpan layers as determined from cone index data. *Agric. Eng. Int. CIGR J.* **2008**, *X*, 1–17.

Disclaimer/Publisher’s Note: The statements, opinions and data contained in all publications are solely those of the individual author(s) and contributor(s) and not of MDPI and/or the editor(s). MDPI and/or the editor(s) disclaim responsibility for any injury to people or property resulting from any ideas, methods, instructions or products referred to in the content.